SIAM J. NUMER. ANAL.
Vol. 61, No. 1, pp. 110-134

LOG ORTHOGONAL FUNCTIONS IN SEMI-INFINITE INTERVALS: APPROXIMATION RESULTS AND APPLICATIONS*

SHENG CHEN† AND JIE SHEN‡

Abstract. We construct two new classes of log orthogonal functions in semi-infinite intervals, log orthogonal functions (LOFs-II) and generalized log orthogonal functions (GLOFs-II), by applying a suitable log mapping to Laguerre polynomials. We develop basic approximation theory for these new orthogonal functions and show that they can provide uniformly good exponential convergence rates for problems in semi-infinite intervals with slow decay at infinity. We apply them to solve several linear and nonlinear differential equations whose solutions decay algebraically or exponentially with very slow rates, and we present ample numerical results to show the effectiveness of the approximations by LOFs-II and GLOFs-II.

Key words. log orthogonal functions, Laguerre polynomials/functions, mapped spectral methods, semi-infinite intervals, exponential convergence

MSC codes. 65N35, 65E05, 65M70, 41A05, 41A10, 41A25

DOI. 10.1137/21M1466840

1. Introduction.

Solutions to many scientific and engineering problems set in unbounded domains exhibit slow decay at infinity. It is notoriously difficult to approximate such functions efficiently without explicit knowledge of their asymptotic behaviors. We consider in this paper approximations of functions on semi-infinite intervals, such as $[a, +\infty)$ or $(-\infty, a]$, with slow or algebraic decay at infinity. For functions with exponential or rapid decay at infinity, the most natural approach is to use the classical Laguerre polynomials/functions which are mutually orthogonal in suitably weighted L^2 spaces. However, it is well known that the classical Laguerre polynomials/functions are not the most efficient due to their poor resolution or approximation properties [5, 32]. Various alternative approaches have been proposed in the past several decades. Within the framework of spectral methods, some of the most popular approaches are as follows:

- Domain mapping [18]: Map the infinite intervals to a bounded interval, and then use standard spectral methods to solve the mapped problems in the bounded interval. The main advantage of this approach is that standard spectral methods can be used, but a disadvantage is the mapped problems can be very complicated, leading to difficulties in analysis and implementation.
- Mapped orthogonal polynomials/functions [8]: Use a suitable mapping to map the classical Jacobi polynomials to mapped orthogonal systems in infinite intervals. To use this approach, one has to develop a complete set of

* Received by the editors December 21, 2021; accepted for publication (in revised form) September 6, 2022; published electronically February 23, 2023.
https://doi.org/10.1137/21M1466840
Funding: The work was partially supported by the National Natural Science Foundation of China grants 11971407 and 11801235, the National Science Foundation grant DMS-2012585, and the AFOSR grant FA9550-20-1-0309.

† Advanced Institute of Natural Sciences, Beijing Normal University, Zhuhai 519087, China (shengchen@bnu.edu.cn).
‡ Corresponding author. Department of Mathematics, Purdue University, West Lafayette, IN 47907-1957 USA (shen7@purdue.edu).

theoretical results and practical tools for the mapped orthogonal polynomials/functions, including new approximation theory, corresponding quadrature formulae, and recurrence relations. Once these tools and results are available, one can use them to solve problems in infinite intervals directly.

- The sinc method [36]: The sinc function is defined as $sinc(x) = \frac{\sin(\pi x)}{\pi x}$. With a suitable transform, the sinc function can be used to approximate problems in $(-\infty, \infty)$ and in $(0, \infty)$ [35, 39].

The first two approaches are mathematically equivalent but lead to different implementation and analysis. The second approach is now widely used, as theoretical results and practical tools for many popular mappings are already available [8, 21, 32, 33]. In particular, the mapped Chebyshev method [5, 21, 32] has been frequently used in practice due to the fact that (i) it provides a faster convergence rate than the Laguerre spectral method, and (ii) fast Fourier transform (FFT) can be used in the implementation. We refer the reader to [5, 21, 32] for more details on the analysis and applications of the mapped Chebyshev method. However, for problems with algebraic decay such as $u(x) \approx x^{-r}$ with noninteger r, the mapped Chebychev method can only converge at an algebraic rate, and the convergence becomes very slow when $0 < r \ll 1$. On the other hand, the sinc method is a particularly powerful approximation method for weakly singular functions and, with a suitable mapping, can lead to exponential convergence for problems with algebraic decay [35, 39].

In our previous work [10], we constructed two new classes of log orthogonal functions (LOFs and GLOFs) in $[0, 1]$ to deal with problems which exhibit weakly singular behaviors at the initial time for initial value problems or at one endpoint for boundary value problems. In particular, LOFs and GLOFs provide very accurate approximation for functions behaving like $t^r(-\log t)^k$ near $t = 0$ for small but positive r. This success motivates us to seek suitable mappings which would allow us to construct orthogonal functions which can provide uniformly good approximation for problems with algebraic decay such as $u(x) \approx x^{-r}$ for a wide range of $r > 0$.

The main purpose of this paper is to construct two new classes of log orthogonal functions in semi-infinite intervals, LOFs-II and GLOFs-II, by applying a suitable log mapping to Laguerre polynomials. We develop basic approximation theory for these new orthogonal functions and show that they can provide uniformly good exponential convergence rates for problems in semi-infinite intervals with algebraic decay (i.e., behaving like x^{-r} as $x \to \infty$) or with exponential decays at very slow rates (i.e., behaving like $\exp(-rx)$ with $0 < r \ll 1$ as $x \to \infty$). Hence, these new log orthogonal functions are particularly useful for problems with slow asymptotic decay rates that cannot be determined a priori.

As applications, we solve the modified Helmholtz equation on the semi-infinite interval and carry out a complete analysis for the weighted Galerkin approximation based on GLOFs-II. We then propose a weighted formulation for a class of fractional differential equations, and finally we solve the nonlinear Thomas–Fermi equation by constructing a suitable weighted approximation based on GLOFs-II. Our numerical results indicate that the new sets of log orthogonal functions are very effective in approximating functions with slow decays at infinity.

The rest of the paper is organized as follows. In the next section, we review some basic results about Laguerre approximations and show that they are not effective for problems with slow decays or fast exponential decay at infinity. In sections 3 and 4, we construct, respectively, the first and second new class of log orthogonal functions (LOFs-II and GLOFs-II) and derive their approximation properties. In sections 5,

6, and 7, we apply GLOFs-II to solve the modified Helmholtz equation, a fractional differential equation, and the nonlinear Thomas–Fermi equation, respectively. Some concluding remarks are given in section 8, and MATLAB codes for evaluating GLOFs-II and the corresponding Gauss quadrature nodes and weights are provided in the appendix.

2. Approximation by Laguerre polynomials/functions. The Laguerre polynomials/functions play a critical role in constructing our new basis functions. We review some of their main properties in this section. In particular, we describe the classical Laguerre approximation theory and explain the inefficiency of the Laguerre approximation to functions which commonly appear in unbounded partial differential equations (PDEs), with algebraic decay or with very large or small exponential delay rate, i.e., $e^{-\lambda y}$ when λ is tiny or large. We refer the reader to [32, 37] for a more detailed study on the Laguerre polynomials/functions.

We start with some notation. Let $(\cdot,\cdot)$ and $\|\cdot\|$ denote the usual inner product and norm in $L^2(\mathbb{R}^+)$, and for a given weight function $\omega > 0$, we denote by $(\cdot,\cdot)_\omega$ and $\|\cdot\|_\omega$ the weighted inner product and norm in $L^2_\omega(\mathbb{R}^+)$. We also denote by $\|\cdot\|_\infty$ the L^∞-norm.

2.1. Laguerre polynomials/functions. The Laguerre polynomials with real parameter $\alpha > -1$ can be defined by the *Rodrigues formula*

$$L_n^{(\alpha)}(y) = \frac{y^{-\alpha}e^y}{n!}\frac{\mathrm{d}^n}{\mathrm{d}y^n}\big(y^{n+\alpha}e^{-y}\big), \quad y \in \mathbb{R}^+,$$

or the *three-term recurrence,* which is more suitable for practical computation:

$$\begin{aligned} &L_0^{(\alpha)}(y) = 1, \quad L_1^{(\alpha)} = -y + \alpha + 1, \\ &L_{n+1}^{(\alpha)}(y) = \frac{2n+\alpha+1-y}{n+1}L_n^{(\alpha)}(y) - \frac{n+\alpha}{n+1}L_{n-1}^{(\alpha)}(y). \end{aligned}$$

They are mutually orthogonal with respect to the weight function $\omega^\alpha(y) = y^\alpha e^{-y}$,

$$\int_0^\infty L_n^{(\alpha)}(y)\, L_m^{(\alpha)}(y)\, y^\alpha e^{-y}\,\mathrm{d}y = \gamma_n^\alpha\,\delta_{mn}, \quad \gamma_n^\alpha = \frac{\Gamma(n+\alpha+1)}{\Gamma(n+1)}. \tag{2.1}$$

For the theoretical analysis and numerical implementation of Laguerre spectral methods, the following *derivative relations* are indispensable:

$$L_n^{(\alpha)}(y) = \partial_y L_n^{(\alpha)}(y) - \partial_y L_{n+1}^{(\alpha)}(y),$$

$$y\partial_y L_n^{(\alpha)}(y) = nL_n^{(\alpha)}(y) - (n+\alpha)L_{n-1}^{(\alpha)}(y),$$

$$\partial_y L_n^{(\alpha)}(y) = -L_{n-1}^{(\alpha+1)}(y) = -\sum_{k=0}^{n-1} L_k^{(\alpha)}(y).$$

The following formula relates the Laguerre polynomials with parameters α and $\alpha+1$:

$$yL_n^{(\alpha+1)}(y) = (n+1+\alpha)L_n^{(\alpha)}(y) - (n+1)L_{n+1}^{(\alpha)}(y).$$

Let $\{y_j^{(\alpha)}\}_{j=0}^N$ be the roots of $L_{n+1}^{(\alpha)}(y)$; then the associated weights are given by

$$\omega_j^{(\alpha)} = \frac{\Gamma(N+\alpha+1)}{(N+\alpha+1)(N+1)!}\frac{y_j^{(\alpha)}}{[L_N^{(\alpha)}(y_j^{(\alpha)})]^2}, \quad 0 \le j \le N, \tag{2.2}$$

and we have the following *Laguerre–Gauss quadrature*:

$$\int_{\mathbb{R}^+} p(y)y^\alpha e^{-y}dy = \sum_{j=0}^N p(y_j^{(\alpha)})\omega_j^{(\alpha)} \quad \forall p(y) \in P_{2N+1}(\mathbb{R}^+). \tag{2.3}$$

On the other hand, the Laguerre functions, which are more suitable for approximations at infinity, are defined by $\widehat{L}_n^{(\alpha)}(y) = e^{-y/2}L_n^{(\alpha)}(y)$. We define the projection operator Π_N^α from $L^2_{y^\alpha}(\mathbb{R}^+)$ to $\hat{P}_N := \{e^{-y/2}p\colon\ p \in P_N\}$ by

$$(\Pi_N^\alpha u - u, v_N)_{y^\alpha} = 0 \quad \forall v_N \in \hat{P}_N,$$

which results in

$$u = \sum_{n=0}^\infty \hat{u}_n \widehat{L}_n^{(\alpha)}, \quad \Pi_N^\alpha u = \sum_{n=0}^N \hat{u}_n \widehat{L}_n^{(\alpha)}, \quad \hat{u}_n = \frac{1}{\gamma_n^\alpha}\int_{\mathbb{R}^+} u(y)\widehat{L}_n^{(\alpha)}(y)y^\alpha \mathrm{d}y. \tag{2.4}$$

PROPOSITION 2.1. *Let* $\hat{\partial}_y = \partial_y + 1/2$ *and* $0 \le m \le N+1$. *If* $\hat{\partial}_y^k u \in L^2_{y^{\alpha+k}}(\mathbb{R}^+)$, $k = 0, 1, \ldots m$, *then*

$$\|\Pi_N^\alpha u - u\|_{y^\alpha} \le cN^{-m/2}\|\hat{\partial}_y^m u\|_{y^{\alpha+m}}, \tag{2.5}$$

where c *is a positive constant independent of* m, N, *and* u.

2.2. Approximation to exponential decay functions. The above error estimate indicates that the convergence rate of the Laguerre approximation relies on the degree of freedom N and the regularity of the underlying functions u in terms of the pseudo-derivative $\partial_y + 1/2$. It has been verified that Laguerre functions are capable of approximating the exponential function $e^{-\lambda y}$ since $N^{-m/2}\|\hat{\partial}_y^m e^{-\lambda y}\|_{y^{\alpha+m}}$ goes to zero exponentially. We provide a precise error estimate for the projection $\Pi_N u := \Pi_N^0 u$ to exponential decay functions below.

PROPOSITION 2.2. *If* $u(x) = e^{-\lambda y}$ *with* $\lambda > 0$, *then*

$$\|\Pi_N u - u\| \le \frac{1}{\sqrt{2\lambda}}(R_\lambda)^{N+1}, \qquad \|\Pi_N u - u\|_\infty \le (R_\lambda)^{N+1},$$

where $R_\lambda = \left|\frac{\lambda - 1/2}{\lambda + 1/2}\right| < 1$ *and* $R_\lambda \approx 1$ *as* $\lambda \to 0$ *or* ∞.

Proof. Using (2.4) and the Rodrigues formula, we find

$$\begin{aligned}\hat{u}_n &= \frac{1}{\gamma_n^0}\int_{\mathbb{R}^+} u(y)\widehat{L}_n^{(0)}(y)\mathrm{d}y = \frac{1}{n!}\int_{\mathbb{R}^+} e^{(1/2-\lambda)y}\frac{\mathrm{d}^n}{\mathrm{d}y^n}\left(y^n e^{-y}\right)\mathrm{d}y \\ &= \frac{(\lambda-1/2)^n}{n!}\int_{\mathbb{R}^+} y^n e^{-(\lambda+1/2)y}\mathrm{d}y = \frac{1}{\lambda+1/2}\left(\frac{\lambda-1/2}{\lambda+1/2}\right)^n.\end{aligned}$$

Then using the orthogonality of the Laguerre functions and the fact that $|L_n^{(0)}| \leq 1$ (see [1, 32]), we obtain

$$\|\Pi_N u - u\| = \left(\sum_{N+1}^{\infty} |\hat{u}_n|^2\right)^{1/2} \leq \frac{1}{\sqrt{2\lambda}} \left|\frac{\lambda - 1/2}{\lambda + 1/2}\right|^{N+1},$$
$$\|\Pi_N u - u\|_\infty \leq \sum_{N+1}^{\infty} |\hat{u}_n| = \left|\frac{\lambda - 1/2}{\lambda + 1/2}\right|^{N+1},$$

which completes the proof. ∎

The above estimate indicates that it is not efficient to approximate functions behaving like $e^{-\lambda x}$ with large or tiny λ at infinity by Laguerre functions.

2.3. Approximation to algebraic decay functions. Another class of functions that frequently appears in solving unbounded PDEs is functions with algebraic decay at infinity. Different from the exponential function $e^{-\lambda x}$, which is smooth in terms of the pseudo-derivative $\hat{\partial}_y = \partial_y + 1/2$, the regularity of the algebraic decay function in terms of the pseudo-derivative $\hat{\partial}_y$ is limited in the space $L^2_{y^{m+\alpha}}(\mathbb{R}^+)$. In fact, for $u(y) \approx y^{-r}$, $y \to \infty$, it holds that

$$\hat{\partial}_y^m u(y) = 2^{-m} u(y) + \sum\nolimits_{k=1}^{m} c_k \partial_y^k u(y) \approx y^{-r} \text{ as } y \to \infty,$$

which means that $\|\hat{\partial}_y^m u\|_{y^{\alpha+m}} < \infty$ if and only if $m < 2r - \alpha - 1$. Hence, we derive from (2.5) that the convergence rate of the approximation by Laguerre functions to $u(y) \approx y^{-r}$, $y \to \infty$ is only $m/2 = r - (\alpha + 1)/2$, which means that the Laguerre approximation is not efficient for functions with slow algebraic decay at infinity.

To illustrate the above theoretical results, we plot the convergence curves of the L^2 projection $\Pi_N u$ to functions $e^{-\lambda y}$ and $(1+y)^{-r}$ on the left and right of Figure 2.1, respectively. The error curves demonstrate that the Laguerre functions are not efficient to approximate $e^{-\lambda y}$ with λ tiny or large, or the function $(1+y)^{-r}$ with small $r > 0$, but can provide good approximations to functions with exponential/algebraic decay functions outside these parameter ranges.

3. Log orthogonal functions for semi-unbounded intervals (LOFs-II). We demonstrated in the last section that the popular Laguerre functions do not provide a uniformly good approximation to functions with algebraic/exponential decay.

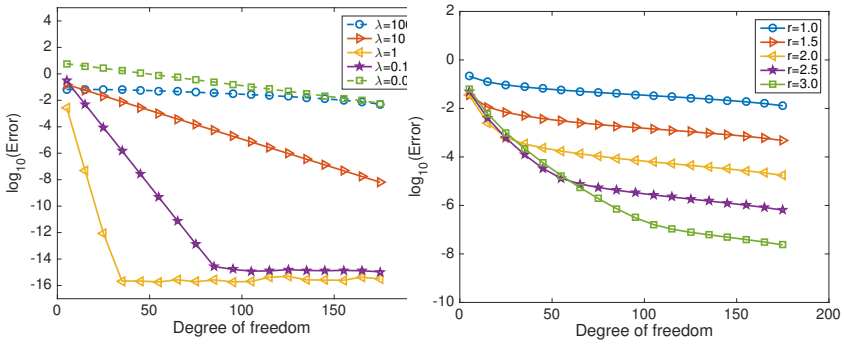

FIG. 2.1. *Convergence curves of Laguerre approximation. Left:* $e^{-\lambda y}$. *Right:* $(1+y)^{-r}$.

We construct new basis functions in this section which are capable of providing uniformly good approximation to all functions which behave like $e^{-\lambda y}$ with $\lambda > 0$ or $(1+y)^{-r}$ with $r > 0$ at infinity.

We first introduce some basic notation.

Domain	$\Lambda = [1, \infty)$
Log mapping	$y = \log x,\ x \in \Lambda$
Parameters	$\alpha > -1, \quad \beta > 1$
Log orthogonal function (LOFS − II)	$\mathcal{U}_n^{(\alpha)}(x) = e^{-y} L_n^{(\alpha)}(y)$
LOFs − II with scaling factor β	$\mathcal{U}_n^{\alpha,\beta}(x) = x^{\beta} \mathcal{U}_n^{(\alpha)}(x^{2\beta})$
Generalized derivatives	$\mathcal{D}_\beta = (2\beta)^{-1} x^{\beta+1} \partial_x (x^{-\beta} u), \quad \mathcal{D} = x\partial_x$
Weight functions	$\chi^\alpha(x) = (\log x)^\alpha,\ \chi^{\alpha,\beta}(x) = x^{-1}(2\beta \log x)^\alpha$

DEFINITION 3.1 (LOFs-II). *Let $\alpha > -1$. The log orthogonal functions for semi-unbounded intervals (LOFs-II) are defined as follows:*

$$\mathcal{U}_n^{(\alpha)}(x) = e^{-y} L_n^{(\alpha)}(y) = x^{-1} L_n^{(\alpha)}(\log x), \quad x \in \Lambda := [1, \infty), \tag{3.1}$$

where $L_n^{(\alpha)}(y)$, $n \geq 0$, are the classical Laguerre polynomials.

From the properties of Laguerre polynomials listed in section 2.1, we can derive the following basic properties of LOFs-II:

- *Orthogonality.* Denoting weight function $\chi^\alpha(x) = (\log x)^\alpha$, it holds that

$$\int_1^\infty \mathcal{U}_n^{(\alpha)}(x)\, \mathcal{U}_m^{(\alpha)}(x)\, \chi^\alpha(x) \mathrm{d}x = \gamma_n^{(\alpha)} \delta_{nm}, \quad \gamma_n^{(\alpha)} := \frac{\Gamma(n+1+\alpha)}{\Gamma(n+1)}. \tag{3.2}$$

- *The three-term recurrence.* Via the mapping $y = \log x$, $x \in [1, \infty)$, it is straightforward to derive that

$$\begin{aligned} &\mathcal{U}_0^{(\alpha)}(x) = 1/x, \quad \mathcal{U}_1^{(\alpha)}(x) = (-\log x + \alpha + 1)/x, \\ &\mathcal{U}_{n+1}^{(\alpha)}(x) = \frac{2n+\alpha+1-\log x}{n+1} \mathcal{U}_n^{(\alpha)}(x) - \frac{n+\alpha}{n+1} \mathcal{U}_{n-1}^{(\alpha)}(x). \end{aligned} \tag{3.3}$$

- *Gauss quadrature formula.* Let $\{\xi_j^{(\alpha)}\}_{j=0}^N$ be the roots of $\mathcal{U}_{N+1}^{(\alpha)}(x)$. Then

$$\int_\Lambda p(x)(\log x)^\alpha \mathrm{d}x = \sum_{j=0}^{N+1} p(\xi_j^{(\alpha)}) \chi_j^{(\alpha)} \quad \forall p \in U_{2N+1} := \mathrm{span}\{\mathcal{U}_n^{(\alpha)}\}_{n=0}^{2N+1}, \tag{3.4}$$

  where the Gauss nodes and weights can be computed from (2.2) and (2.3),

$$\xi_j^{(\alpha)} = e^{y_j^{(\alpha)}}, \quad \chi_j^{(\alpha)} = (\xi_j^{(\alpha)})^2 \omega_j^{(\alpha)}; \tag{3.5}$$

  here $\{y_j^{(\alpha)}, \omega_j^{(\alpha)}\}_{j=0}^N$ are the pairs of the zeros and weights of $L_{N+1}^{(\alpha)}(y)$.

- *Derivative relation I.* Referring to [11, eq. (2.45)], [29, eq. (6.146)], or [30, eq. (B-7.2)], we know that

$$\partial_y \big(e^{-y} L_n^{(\alpha)}(y)\big) = -e^{-y} L_n^{(\alpha+1)}(y).$$

Then we have the following derivative relation by the chain rule:

$$x \partial_x \mathcal{U}_n^{(\alpha)}(x) = \partial_y \big(e^{-y} L_n^{(\alpha)}(y)\big) = -\mathcal{U}_n^{(\alpha+1)}(x).$$

Repeating the above relation leads to

$$\mathcal{D}^k \mathcal{U}_n^{(\alpha)}(x) = (-1)^k \mathcal{U}_n^{(\alpha+k)}(x), \quad k = 0, 1, 2, \ldots. \tag{3.6}$$

- *Derivative relation II.* Using the relation [11, eq. (2.46)] and the chain rule yields

$$\mathcal{D}\big(\log x\, \mathcal{U}_n^{(1)}(x)\big) = (n+1)\mathcal{U}_{n+1}^{(0)}(x). \tag{3.7}$$

- *Rodrigues-like formula.*

$$\mathcal{U}_n^{(\alpha)}(x) = (\log x)^{-\alpha} \mathcal{D}^n \big\{(\log x)^{n+\alpha} x^{-1}\big\}/n!. \tag{3.8}$$

To better describe the approximation ability of the log orthogonal functions, we define the following weighted Hilbert space:

$$A_\alpha^m(\Lambda) := \big\{v \in L^2_{\chi^\alpha}(\Lambda):\ \mathcal{D}^k v \in L^2_{\chi^{\alpha+k}}(\Lambda),\ k = 1, 2, \ldots, m\big\}, \quad \chi^\beta(x) = (\log x)^\beta, \tag{3.9}$$

and we denote by π_N^α the projection operator from $L^2_{\chi^\alpha}$ to $U_N = \mathrm{span}\{\mathcal{U}_n^{(\alpha)}\}_{n=0}^N$ such that

$$(\pi_N^\alpha u - u, v)_{\chi^\alpha} = 0 \ \ \forall\, v \in U_N,$$

where the superscript of the projector π_N^α may be dropped whenever $\alpha = 0$.

THEOREM 3.1. *Let $\alpha > -1$ and $0 \le k \le m$. For any $u \in A_\alpha^m(\Lambda)$, we have*

$$\|\mathcal{D}^k(\pi_N^\alpha u - u)\|_{\chi^{\alpha+k}} \le \sqrt{\frac{\Gamma(N+2+\alpha+k)}{\Gamma(N+2+\alpha+m)}}\|\mathcal{D}^m u\|_{\chi^{\alpha+m}} \le c N^{\frac{k-m}{2}} \|\mathcal{D}^m u\|_{\chi^{\alpha+m}}, \tag{3.10}$$

where the positive constant $c \approx 1$ for $N \gg 1$.

Proof. Since $u \in L^2_{\chi^\alpha}(\Lambda)$, we can write

$$u(x) = \sum_{n=0}^\infty \tilde{u}_n \mathcal{U}_n^{(\alpha)}(x), \quad \pi_N^\alpha u(x) = \sum_{n=0}^N \tilde{u}_n \mathcal{U}_n^{(\alpha)}(x).$$

Then, for any $u \in A_\alpha^m(\Lambda)$, by the orthogonality (3.2) and the derivative relation (3.6), it holds that

$$\begin{aligned} \|\mathcal{D}^k(\pi_N^\alpha u - u)\|^2_{\chi^{\alpha+k}} &= \sum_{n=N+1}^\infty |\tilde{u}_n|^2 \int_1^\infty \big(\mathcal{U}_n^{(\alpha+k)}(x)\big)^2 \chi^{\alpha+k}(x)\mathrm{d}x \\ &= \sum_{n=N+1}^\infty |\tilde{u}_n|^2 \gamma_n^{(\alpha+k)} \le \frac{\gamma_{N+1}^{(\alpha+k)}}{\gamma_{N+1}^{(\alpha+m)}} \sum_{n=N+1}^\infty |\tilde{u}_n|^2 \gamma_n^{(\alpha+m)} \\ &\le \frac{\Gamma(N+2+\alpha+k)}{\Gamma(N+2+\alpha+m)} \|\mathcal{D}^m u\|^2_{\chi^{\alpha+m}}. \end{aligned} \tag{3.11}$$

We recall the following useful result: for any constant $a, b \in \mathbb{R}$, $n \in \mathbb{N}$, $n + a > 1$, and $n + b > 1$ (see [43, Lemma 2.1]),

$$\frac{\Gamma(n+a)}{\Gamma(n+b)} \le \nu_n^{a,b} n^{a-b}, \tag{3.12}$$

where $\nu_n^{a,b} \approx 1$ for $n \gg 1$ owing to

$$\nu_n^{a,b} = \exp\left(\frac{a-b}{2(n+b-1)} + \frac{1}{12(n+a-1)} + \frac{(a-b)^2}{n}\right). \tag{3.13}$$

We can then complete the proof by applying (3.12) to (3.11). ∎

COROLLARY 3.1. *For any $u \in A_0^m(\Lambda)$, we have*

$$\|\pi_N u - u\| \le \sqrt{\frac{\Gamma(N+2+k)}{\Gamma(N+2+m)}}\|\mathcal{D}^m u\|_{\chi^m} \le cN^{-\frac{m}{2}}\|\mathcal{D}^m u\|_{\chi^m}. \tag{3.14}$$

Moreover, for the algebraic decay function x^{-r} with $r > 1/2$, we have

$$\|\pi_N u - u\| \le c\,[2\pi eN/r]^{1/4}\,2^{-[eN/r]/2}, \tag{3.15}$$

where the positive constant $c \approx 1$ for $N \gg 1$.

Proof. Taking $\alpha = 0$ and $k = 0$ in (3.10), we obtain (3.14). On the other hand, for $r > 1/2$ (which is necessary for $x^{-r} \in L^2(\mathbb{R}^+)$), we have

$$\|\mathcal{D}^m x^{-r}\|_{\chi^m}^2 = \int_1^\infty \left(\mathcal{D}^m x^{-r}\right)^2 (\log x)^m \mathrm{d}x = r^{2m}\int_0^\infty e^{-2ry} y^m \mathrm{d}y = \frac{r^{2m}\,\Gamma(m+1)}{(2r)^{m+1}}.$$

Thanks to the following property of the Gamma function (see [1, eq. (6.1.38)]),

$$\Gamma(z+1) = \sqrt{2\pi} z^{z+\frac{1}{2}} \exp\left(-z + \frac{\theta}{12z}\right), \quad 0 < \theta < 1 \quad \forall z > 0, \tag{3.16}$$

we find that for any integer $m > 0$,

$$N^{-\frac{m}{2}}\|\mathcal{D}^m u\|_{\chi^m} = \exp\left(\frac{\theta}{12m}\right)\,(2\pi m)^{1/4}\left(\frac{rm}{2eN}\right)^{m/2}.$$

Hence, by taking $m = [eN/r]$, we obtain

$$\|\pi_N x^{-r} - x^{-r}\| \le c\,[2\pi eN/r]^{1/4}\,2^{-[eN/r]/2}. \tag{3.17}$$

∎

The above result indicates that the approximation by LOFs-II for $u = x^{-r}$ converges exponentially for all $r > 1/2$.

4. Generalized log orthogonal functions for semi-unbounded intervals (GLOFs-II). As with all other spectral methods in unbounded domain, the performance of LOF-II approximations can be improved with a scaling factor. To further understand the role of the mapping $y = \log x$, we plot, on the left of Figure 4.1, the roots of the LOFs-II with $n = 10, 30, 50, 70, 90$, and, on the right of Figure 4.1, the LOFs-II with $n = 10, 90$. We observe from the left figure that the roots of the LOFs-II increase extremely quickly with n. This seriously affects the quality of the approximation by LOFs-II as many nodes with large x values maybe wasted.

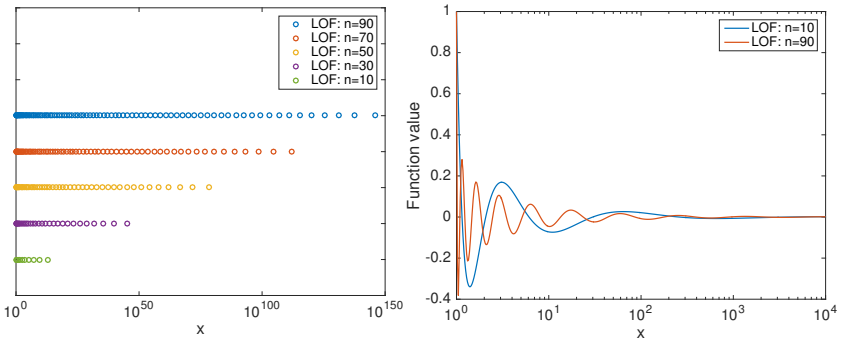

FIG. 4.1. *Left: Nodes distribution. Right: LOFs-II.*

4.1. Definition and basic properties.

DEFINITION 4.1 (GLOFs-II). *Let $\alpha > -1$ and $\beta > 1$. The generalized log orthogonal functions for semi-unbounded intervals (GLOFs-II) are defined as follows:*

$$\mathcal{U}_n^{\alpha,\beta}(x) := \mathcal{U}_n^{(\alpha)}(\beta, x) = x^{\beta}\mathcal{U}_n^{(\alpha)}(x^{2\beta}) = x^{-\beta}L_n^{(\alpha)}(\log x^{2\beta}), \tag{4.1}$$

where the variable $x \in \Lambda := [1, \infty)$.

The GLOFs-II bring in not only the scaling factor β but also an extra multiplier x^{β} to ensure that $\{\mathcal{U}_n^{\alpha,\beta}(x)\}_{n=0}^{\infty}$ are dense in

$$L^2_{\chi^{\alpha,\beta}}(\Lambda),\ \chi^{\alpha,\beta}(x) = x^{-1}(2\beta\log x)^{\alpha}.$$

Hence they can provide good approximation to x^{-r} for all $r > 0$, extending the restriction $r > 1/2$ for $\{\mathcal{U}_n^{(\alpha)}(x)\}_{n=0}^{\infty}$ which is dense in $L^2_{\chi^{\alpha}}(\Lambda) \subset L^2_{\chi^{\alpha,\beta}}(\Lambda)$.

In view of the benefits from the scaling factor β and the multiplier x^{β}, it is more suitable to use GLOFs-II $\mathcal{U}_n^{\alpha,\beta}(x)$ for practical computations.

We list below the basic properties of GLOFs-II $\mathcal{U}_n^{\alpha,\beta}(x)$:

(i) Using the orthogonality

$$\int_1^{\infty} \mathcal{U}_n^{\alpha,\beta}(x)\,\mathcal{U}_m^{\alpha,\beta}(x)\,\chi^{\alpha,\beta}(x)\mathrm{d}x = \gamma_n^{\alpha,\beta}\delta_{nm}, \quad \gamma_n^{\alpha,\beta} := \frac{\Gamma(n+1+\alpha)}{2\beta\,\Gamma(n+1)}, \tag{4.2}$$

any $u \in L^2_{\chi^{\alpha,\beta}}(\Lambda)$ can be expanded as

$$u(x) = \sum_{n=0}^{\infty} \hat{u}_n \mathcal{U}_n^{\alpha,\beta}(x), \quad \hat{u}_n = \frac{1}{\gamma_n^{\alpha,\beta}} \int_{\Lambda} u(x)\,\mathcal{U}_n^{\alpha,\beta}(x)\,\chi^{\alpha,\beta}(x)\mathrm{d}x. \tag{4.3}$$

(ii) The related Gauss quadrature formula is

$$\int_{\Lambda} f(x)\,\chi^{\alpha,\beta}(x)\,\mathrm{d}x \approx \sum_{j=0}^{N+1} f(\xi_j^{\alpha,\beta})\chi_j^{\alpha,\beta}, \quad \chi^{\alpha,\beta}(x) = x^{-1}(2\beta\log x)^{\alpha}, \tag{4.4}$$

where the Gauss nodes and weights are

$$\xi_j^{\alpha,\beta} = \sqrt[2\beta]{\xi_j^{(\alpha)}}, \quad \chi_j^{\alpha,\beta} = [2\beta(\xi_j^{\alpha,\beta})^{2\beta}]^{-1}\,\chi_j^{(\alpha)}.$$

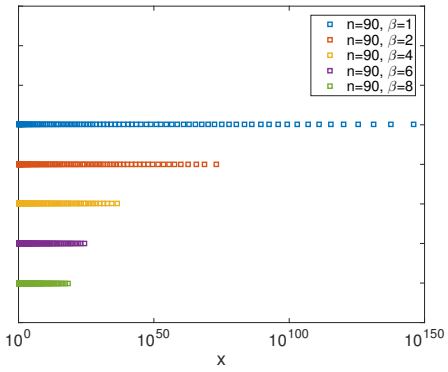

FIG. 4.2. *Nodes distribution with difference scaling parameter* β.

We derive from the above that

$$\int_\Lambda f(x)\,\mathrm{d}x = \int_\Lambda \frac{f(x)}{\chi^{\alpha,\beta}(x)}\chi^{\alpha,\beta}(x)\,\mathrm{d}x \approx \sum_{j=0}^{N+1} \frac{f(\xi_j^{\alpha,\beta})}{\chi^{\alpha,\beta}(\xi_j^{\alpha,\beta})}\chi_j^{\alpha,\beta}.$$

We observe from the above that the log-Gaussian quadrature nodes and weights can be computed by using the Laguerre quadrature formula in [32, section 7.1.2]. MATLAB code for computing the log-Gaussian quadrature nodes and weights is provided in the appendix. In Figure 4.2, we plot the log-Gaussian quadrature nodes with $n = 90$ and different β, and we observe that as β increases, the largest quadrature points rapidly decrease.

(iii) The three-term recurrence is

$$\begin{aligned} &\mathcal{U}_0^{\alpha,\beta}(x) = x^{-\beta}, \quad \mathcal{U}_1^{\alpha,\beta}(x) = x^{-\beta}(\alpha+1-2\beta\log x),\\ &\mathcal{U}_{n+1}^{\alpha,\beta}(x) = \frac{2n+\alpha+1-2\beta\log x}{n+1}\mathcal{U}_n^{\alpha,\beta}(x) - \frac{n+\alpha}{n+1}\mathcal{U}_{n-1}^{\alpha,\beta}(x). \end{aligned} \tag{4.5}$$

(iv) Combining the chain rule with (3.6) and (3.7), we derive the derivative relations

$$\begin{aligned} &\mathcal{D}_\beta^k \mathcal{U}_n^{\alpha,\beta}(x) = (-1)^k \mathcal{U}_n^{\alpha+k,\beta}(x),\\ &\mathcal{D}_\beta\big(\log x\,\mathcal{U}_n^{1,\beta}(x)\big) = \frac{n+1}{2\beta}\,\mathcal{U}_{n+1}^{0,\beta}(x), \end{aligned} \tag{4.6}$$

where the generalized derivative $\mathcal{D}_\beta$ is defined as

$$\mathcal{D}_\beta u := (2\beta)^{-1}x^{\beta+1}\partial_x(x^{-\beta}u) = \frac{1}{2\beta}x\partial_x u - \frac{1}{2}u = \left(\frac{1}{2\beta}\mathcal{D} - \frac{1}{2}\right)u. \tag{4.7}$$

The generalized derivative (4.7) implies that $\partial_x u = \beta x^{-1}(2\mathcal{D}_\beta + 1)u$. Hence

$$\begin{aligned} &\partial_x \mathcal{U}_n^{\alpha,\beta}(x) = \beta x^{-1}\big[\mathcal{U}_n^{\alpha,\beta}(x) - 2\mathcal{U}_n^{\alpha+1,\beta}(x)\big],\\ &\partial_x\big(\log x\,\mathcal{U}_n^{1,\beta}(x)\big) = x^{-1}\big[\beta\log x\,\mathcal{U}_n^{1,\beta}(x) + (n+1)\mathcal{U}_{n+1}^{0,\beta}(x)\big]. \end{aligned} \tag{4.8}$$

(v) Substituting the generalized derivative $x\partial_x u(x^{2\beta}) = 2\beta x^{2\beta}\partial_{x^{2\beta}}u(x^{2\beta})$ into the Rodrigues-like formula (3.8) leads to

$$\mathcal{U}_n^{\alpha,\beta}(x) = x^\beta \mathcal{U}_n^{(\alpha)}(x^{2\beta}) = x^\beta(\log x)^{-\alpha}\,\mathcal{D}^n\big\{(\log x)^{n+\alpha}x^{-2\beta}\big\}/n!. \tag{4.9}$$

Approximation results by the GLOFs-II with scaling factor β can be derived by following a process similar to that in the proof of Theorem 3.1. Indeed, let $\pi_N^{\alpha,\beta}$ be the projection operator from $L^2_{\chi^{\alpha,\beta}}(\Lambda)$ to $U_N^\beta := \text{span}\{\mathcal{U}_n^{\alpha,\beta}\}$ such that

$$\left(\pi_N^{\alpha,\beta}u - u, v\right)_{\chi^{\alpha,\beta}} = 0 \ \ \forall\, v \in U_N^\beta.$$

Then using the same procedure as in the proof of Theorem 3.1, we can derive the following result.

THEOREM 4.1. *Let real $\alpha > -1$, $\beta > 1$, and integers $0 \le k \le m$. Then*

$$\|\mathcal{D}_\beta^k(\pi_N^{\alpha,\beta}u - u)\|_{\chi^{\alpha+k,\beta}} \le cN^{\frac{k-m}{2}}\|\mathcal{D}_\beta^m u\|_{\chi^{\alpha+m,\beta}} \quad \forall u \in \mathcal{H}^m(\Lambda), \tag{4.10}$$

where the positive constant $c \approx 1$ for $N \gg 1$, $\mathcal{D}_\beta u = (2\beta)^{-1}x^{\beta+1}\partial_x(x^{-\beta}u)$, and

$$\mathcal{H}^m(\Lambda) = \left\{v \;\middle|\; x^k\partial_x^k v \in L^2_{\chi^{\alpha+m,\beta}}(\Lambda), \quad k = 0, 1, \ldots m\right\}, \quad m \in \mathbb{N}. \tag{4.11}$$

4.2. Approximation results for some typical functions. The drawback of the Laguerre approximation to exponential functions is exhibited in Proposition 2.2, as it shows that the convergence of the Laguerre projection $\Pi_N e^{-\lambda x}$ to $e^{-\lambda x}$ is very slow when λ is large or tiny. On the other hand, the result in Theorem 4.1 shows that the new basis functions are capable of providing good approximations to a large class of functions in $\mathcal{H}^m(\Lambda)$ which includes the classical Schwartz-space

$$\mathcal{S} = \{v \in C^\infty(\Lambda) |\ \forall\ k, m \in \mathbb{N},\ x^k\partial_x^m v \in C(\Lambda)\}.$$

Note that both exponential decay function $e^{-\lambda x}$, $\lambda > 0$, and algebraic decay function x^{-r}, $r > 0$, are the elements of the space $\mathcal{H}^m(\Lambda)\ \forall m \in \mathbb{N}$. We show below that the approximation by GLOFs-II can provide uniformly good approximation to some typical functions with slow decays at infinity.

Consider first $e^{-\lambda x}$. The relation $\mathcal{D}_\beta^m = \sum_{k=0}^m c_k x^k \partial_x^k$ leads to

$$\mathcal{D}_\beta^m e^{-\lambda x} = \sum_{k=0}^m (-1)^k c_k (\lambda x)^k e^{-\lambda x} \overset{z=\lambda x}{=} \sum\nolimits_{k=0}^m (-1)^k c_k z^k e^{-z},$$

which indicates that the behavior of the function $\mathcal{D}_\beta^m e^{-\lambda x}$ is independent of λ.

Next, we consider the Mittag–Leffler function $E_{\nu,1}(-x^\nu)$, which plays a crucial role in solving fractional differential equations [17, 22, 24]:

$$E_{a,b}(z) = \sum_{j=0}^\infty \frac{z^j}{\Gamma(aj+b)}, \quad z \in \mathbb{C},\ a > 0,\ b \in \mathbb{R}.$$

A direct calculation leads to

$$x^k\partial_x^k E_{\nu,1}(-x^\nu) = x^k\partial_x^k \sum_{j=0}^\infty \frac{(-1)^j x^{j\nu}}{\Gamma(j\nu+1)} = E_{\nu,1-k}(-x^\nu), \quad x > 0.$$

It is shown in [12, Lemma 2.2] that $E_{\nu,1-k}(-x^\nu) \lesssim (1+x^\nu)^{-1}$, $x > 0$, for any non-negative integer k, which implies that $E_{\nu,1}(-x^\nu) \in \mathcal{H}^m(\Lambda)\ \forall m \in \mathbb{N}$. Hence, one can expect that the GLOFs-II approximation to the Mittag–Leffler function $E_{\nu,1}(-x^\nu)$ is exponentially convergent.

In fact, for the the function $u(x) = x^{-r}$ with $r > 0$, we can derive from Theorem 4.1 and the fact that

$$\mathcal{D}_\beta^m x^{-r} = \left(-\frac{\beta + r}{2\beta}\right)^m \; x^{-r}$$

the following explicit rate of exponential convergence.

COROLLARY 4.1. *Let $r > 0$, $\alpha > -1$, $\beta > 1$, and $N > -\alpha/\log\left|\frac{\beta - r}{\beta + r}\right|$. Then for $u(x) = x^{-r}$, $x \in \Lambda = (1, \infty)$, we have*

$$\|\pi_N^{\alpha,\beta} u - u\|_{L^2_{\chi^{\alpha,\beta}}} \le c_{r,1}^{\alpha,\beta} \; (N+1)^\alpha \left|\frac{\beta - r}{\beta + r}\right|^{N+1},$$

where constant $c_{r,1}^{\alpha,\beta}$ is independent of N.

Proof. Since $u \in L^2_{\chi^{\alpha,\beta}}(\Lambda)$, it can be expanded as

$$u = \sum_{n=0}^{\infty} \hat{u}_n \mathcal{U}_n^{\alpha,\beta}, \quad \hat{u}_n = \int_1^\infty u(x) \; \mathcal{U}_n^{\alpha,\beta}(x) \; x^{-1} (2\beta \log x)^\alpha \mathrm{d}x.$$

The coefficient $\hat{u}_n$ can be estimated by the Rodrigues formula (4.9) as follows:

$$\begin{aligned}
\hat{u}_n &= \frac{(2\beta)^\alpha}{n!} \int_1^\infty x^{\beta - r - 1} \; \mathcal{D}^n \left\{ (\log x)^{n+\alpha} x^{-2\beta} \right\} \mathrm{d}x \\
&= \frac{(2\beta)^\alpha}{n!} \int_1^\infty x^{\beta - r} \; (\partial_x x)^n \left\{ (\log x)^{\alpha+n} x^{-2\beta - 1} \right\} \mathrm{d}x \\
&= \frac{(2\beta)^\alpha}{n!} (\beta - r)^n \int_1^\infty x^{-1-r-\beta} (\log x)^{\alpha+n} \; \mathrm{d}x \\
&= \frac{(2\beta)^\alpha}{n!} (\beta - r)^n \int_0^\infty e^{-(\beta+r)y} y^{\alpha+n} \; \mathrm{d}y \\
&= \frac{(2\beta)^\alpha \Gamma(n + \alpha + 1)}{(\beta + r)^{\alpha+1} \Gamma(n+1)} \left(\frac{\beta - r}{\beta + r}\right)^n \\
&\le \frac{(2\beta)^\alpha \nu_n^{\alpha+1,1}}{(\beta + r)^{\alpha+1}} \, n^\alpha \left(\frac{\beta - r}{\beta + r}\right)^n.
\end{aligned}$$

We note that (3.12) is used to derive the last inequality.

Then, for $u = x^{-r}$, it holds that

(1) for $-1 < \alpha \le 0$,

$$\begin{aligned}
\|\pi_N^{\alpha,\beta} u - u\|^2_{L^2_{\chi^{\alpha,\beta}}} &= \sum_{n=N+1}^\infty |\hat{u}_n|^2 \le \left(\frac{(2\beta)^\alpha \nu_n^{\alpha+1,1}}{(\beta + r)^{\alpha+1}} \, (N+1)^\alpha\right)^2 \sum_{n=N+1}^\infty \left|\frac{\beta - r}{\beta + r}\right|^{2n} \\
&\le \left(\frac{(2\beta)^\alpha \nu_n^{\alpha+1,1}}{2\sqrt{\beta r}(\beta + r)^\alpha} \, (N+1)^\alpha \left|\frac{\beta - r}{\beta + r}\right|^{N+1}\right)^2;
\end{aligned}$$

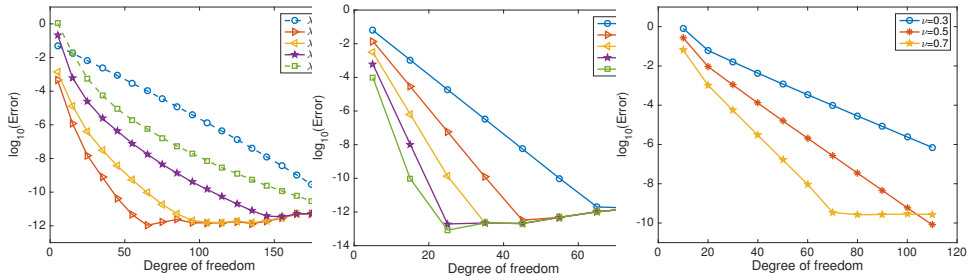

FIG. 4.3. *Convergence curves of log approximations. Left:* $e^{-\lambda x}$. *Middle:* x^{-r}. *Right:* $E_{\nu,1}(-x^{\nu})$.

(2) for $\alpha > 0$, since $n^{2\alpha}|\frac{\beta-r}{\beta+r}|^{2n}$ is monotone decreasing of n when $n > -\alpha/\log|\frac{\beta-r}{\beta+r}|$, it is valid that

$$\begin{aligned}\|\pi_N^{\alpha,\beta}u-u\|^2_{L^2_{\chi^{\alpha,\beta}}} &= \sum_{n=N+1}^{\infty}|\tilde{u}_n|^2 \le \left(\frac{(2\beta)^{\alpha}\nu_n^{\alpha+1,1}}{(\beta+r)^{\alpha+1}}\right)^2 \sum_{n=N+1}^{\infty} n^{2\alpha}\left|\frac{\beta-r}{\beta+r}\right|^{2n}\\ &\le \left(\frac{(2\beta)^{\alpha}\nu_n^{\alpha+1,1}}{(\beta+r)^{\alpha+1}}\right)^2 \int_{N+1}^{\infty} x^{2\alpha}\left|\frac{\beta-r}{\beta+r}\right|^{2x}\mathrm{d}x\\ &\le \left(\frac{(2\beta)^{\alpha}\nu_n^{\alpha+1,1}}{(\beta+r)^{\alpha+1}}\right)^2 \left(2\log\left|\frac{\beta+r}{\beta-r}\right|\right)^{-2\alpha-1} \int_{(N+1)\log|\frac{\beta+r}{\beta-r}|^2}^{\infty} y^{2\alpha}e^{-y}\mathrm{d}y.\end{aligned}$$

Combining the above relations with the asymptotic behavior of the incomplete Gamma function [1, 2, 16]

$$\Gamma(a,X)=\int_X^{\infty} y^{a-1}e^{-y}\mathrm{d}x \approx X^{a-1}e^{-X} \quad \text{for } X \gg 1,$$

we arrive at the desired result. ∎

We now present some numerical experiments to verify the above results. Let $\alpha=0$ and $\beta=5$. The L^2 convergence curves of the LOF approximation $\pi_N^{\alpha,\beta}u$ to exponential decay functions $e^{-\lambda x}$ with $\lambda=100,10,1,0.1,0.01$, algebraic decay functions x^{-r}, $r=1,3/2,2,5/2,3$, and two-parameter Mittag–Leffler functions $E_{\nu,1}(-x^{\nu})$ with $\nu=0.3,0.5,0.7$ are plotted in Figure 4.3. The numerical results demonstrate that both exponential decay functions and algebraic decay functions can be approximated by GLOFs-II very well.

4.3. Comparison between approximations by GLOFs-II and Laguerre functions. In order to compare with the classical Laguerre approximation which is based on Laguerre orthogonal functions $\widehat{L}_n^{(\gamma)}(y)$, $y\in\mathbb{R}^+$, the shifted GLOFs-II $\phi_n(y)=\mathcal{U}_n^{\alpha,\beta}(y+1)$ are applied to approximate functions $e^{-\lambda y}$, $(1+y)^{-r}$, and $E_{s,1}(-(1+y)^s)$. The convergence curves of the approximations by Laguerre functions and by GLOFs-II are plotted in Figure 4.4, where the parameters are set to $\gamma=0$, $\alpha=0$, and $\beta=5$, respectively. We observe that the approximation by GLOFs-II converges exponentially, but approximation by Laguerre functions converges very slowly.

4.4. Comparison with rational approximations. Besides the Laguerre functions, rational orthogonal functions [6, 7, 19, 33, 42] are also frequently used for solving problems defined in semi-infinite domains. We compare below the convergence

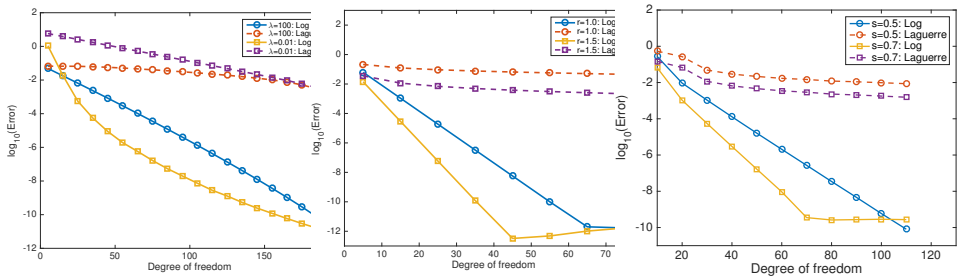

FIG. 4.4. *Convergence comparison: Left:* $e^{-\lambda y}$. *Middle:* $(1+y)^{-r}$. *Right:* $E_{s,1}(-(1+y)^s)$.

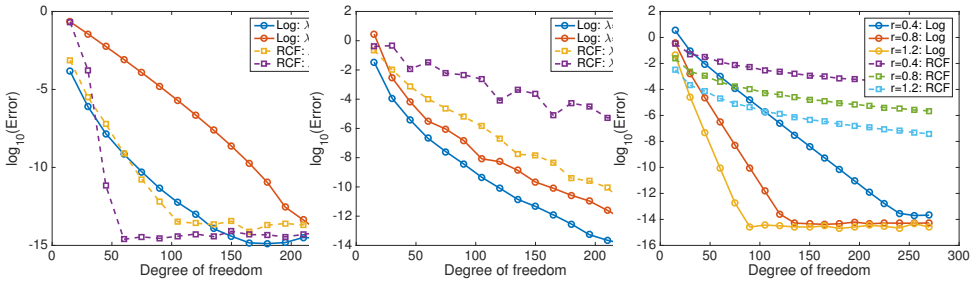

FIG. 4.5. *Convergence curves. Left & middle:* $e^{-\lambda y}$. *Right:* $(1+y)^{-r}$.

rate of the numerical solutions obtained from the shifted GLOFs-II and the rational Chebyshev functions which are most frequently used in practice.

- Shifted GLOFs-II:

$$\phi_n^0(y) = \mathcal{U}_n^{\alpha,\beta}(y+1), \quad y \in [0,\infty). \tag{4.12}$$

- Rational Chebyshev functions (RCFs):

$$R_n^c(y) = T_n\left(\frac{y-1}{y+1}\right), \quad y \in [0,\infty). \tag{4.13}$$

In Figure 4.5 we use GLOFs-II $\mathcal{U}_n^{\alpha,\beta}$ with $\alpha = 0$, $\beta = 5$, and RCFs to approximate the exponential functions $e^{-\lambda y}$ and algebraic decay function $(1+y)^{-r}$ with different $\lambda > 0$ and $r > 0$. We observe that for λ small and noninteger r small, i.e., for functions with slow decays at infinity, the GLOFs-II perform much better than RCFs. However, for functions with fast decay at infinity, the RCF approximation is better than the GLOFs-II.

4.5. Comparison with sinc approximations. We now compare approximations by GLOFs-II with the mapped sinc functions. The sinc function [36] is defined as

$$sinc(w) = \frac{\sin(\pi w)}{\pi w}, \quad w \in \mathbb{C}. \tag{4.14}$$

With the transforms [35, 39]

$$y = \Phi_1(w) = e^w, \quad \Phi_1^{-1}(y) = \log(y),$$
$$y = \Phi_2(w) = e^{\frac{\pi}{2}\sinh\omega}, \quad \Phi_2^{-1}(y) = \sinh^{-1}\left(\frac{2}{\pi}\log y\right),$$

we can approximate a function $f(y)$, $y \in (0,\infty)$, by mapped sinc functions as follows:

$$f(y) \simeq f_{p,N}(y) = \sum_{k=-N/2}^{N/2} f(\Phi_p(kh))\, sinc\big(\Phi_p^{-1}(y)/h - k\big), \quad k \in \mathbb{Z},\ h > 0, \tag{4.15}$$

where h is a parameter depending on N as follows:

$$h = \begin{cases} \sqrt{\pi/N}, & p = 1; \\ \log(\pi/N)/N, & p = 2. \end{cases}$$

It is shown in [28, 38, 39] that approximation errors by these mapped sinc functions decay exponentially for $f(y)$ with algebraic decay—more precisely, if $f(\Phi_p(w))$ is holomorphic on a strip

$$\mathcal{D}_d := \{w \in \mathbb{C} || \operatorname{Im} w | < d\}, \quad 0 < d < \pi,$$

and satisfies the condition

$$|f(z)| \le C \left| \frac{z^r}{(1+z^2)^r} \right|, \quad r > 0.$$

Note that the above condition implies that $f(0) = 0$.

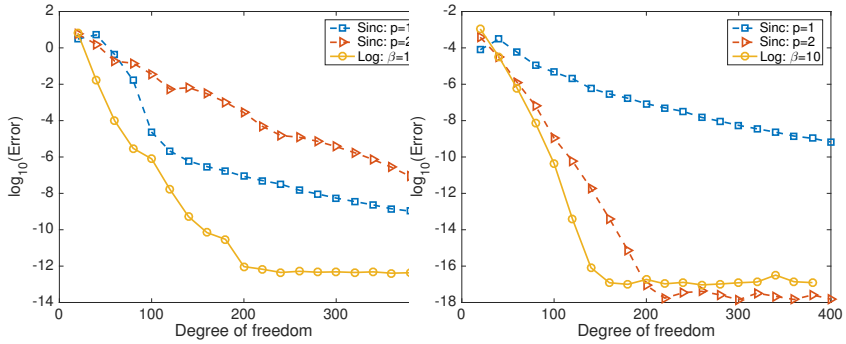

FIG. 4.6. *Convergence curves. Left:* $ye^{-0.01y}$. *Right:* ye^{-100y}.

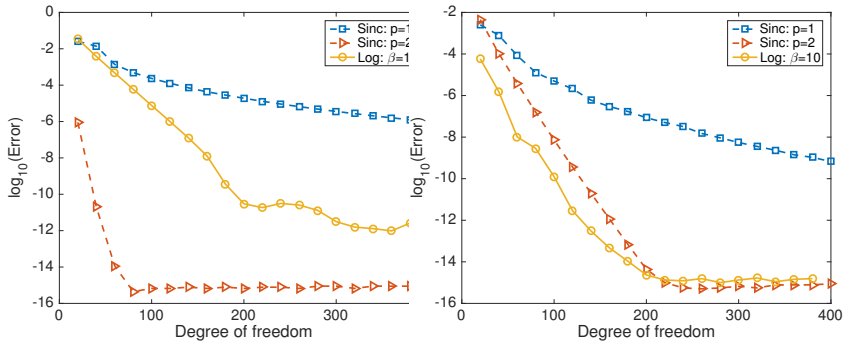

FIG. 4.7. *Convergence curves. Left:* $\frac{y}{1+y^{1.5}}$. *Right:* $\frac{y}{1+y^{3.5}}$.

In order to compare the GLOFs-II with the mapped sinc functions, we plot the errors of the GLOFs-II with $\beta = 10$ and of the mapped sinc approximations in Figures 4.6 and 4.7 for four different functions. We observe that the GLOFs-II approximation is much better than the mapped sinc functions with $p = 1$ in all cases. We also observe from Figure 4.6 that the GLOFs-II provide better approximations than the mapped sinc functions with $p = 2$ for functions with very slow and fast exponential decays. On the other hand, for functions with algebraic decays in Figure 4.7, approximation errors by both the GLOFs-II and the mapped sinc functions with $p = 2$ converge exponentially, and the latter is better for functions at a slower decay rate but a little worse for functions at a slightly faster decay rate.

5. Application to second-order differential equations. In this section, we shall use GLOFs-II to solve a second-order differential equation and establish the basic structure of the numerical analysis, which provides the basic idea for general cases.

5.1. Second-order differential equation. Consider the modified Helmholtz equation

$$-\partial_{xx} u + \lambda^2 u = f, \quad x \in \Lambda = (1, \infty), \tag{5.1}$$

with the homogeneous boundary conditions $u(1) = \lim_{x\to\infty} u(x) = 0$. In order to use GLOFs-II, we use the following weighted weak formulation:
Find $u \in \mathcal{W}_0^1(\Lambda)$ such that

$$a(u, v) := \big(\partial_x u, \partial_x (v x^{-1})\big) + \lambda^2 (u, v)_{x^{-1}} = (f, v)_{x^{-1}} \quad \forall\, v \in \mathcal{W}_0^1(\Lambda), \tag{5.2}$$

where the weighted Sobolev space is defined by

$$\mathcal{W}_0^1(\Lambda) := \Big\{ v x^{-1} \in L_x^2(\Lambda) :\ \partial_x (v x^{-1}) \in L_x^2(\Lambda), \quad v(1) = \lim_{x\to\infty} v(x) = 0 \Big\}$$

equipped with the norm

$$\|v\|_{1,x} = (|v|_{0,x}^2 + |v|_{1,x}^2)^{1/2}, \quad |v|_{k,x} = \left(\int_\Lambda |\partial_x^k (v x^{-1})|^2 \, x \, dx \right)^{1/2}, \ k = 0, 1. \tag{5.3}$$

LEMMA 5.1. *The bilinear form $a(\cdot,\cdot)$ is continuous and coercive in $\mathcal{W}_0^1(\Lambda)$, i.e.,*

$$a(u, v) \le \max\{1, \lambda^2\} \|u\|_{1,x} \|v\|_{1,x}, \quad u,\, v \in \mathcal{W}_0^1(\Lambda); \tag{5.4}$$

$$a(u, u) \ge \min\{1, \lambda^2\} \|u\|_{1,x}^2, \quad u \in \mathcal{W}_0^1(\Lambda). \tag{5.5}$$

Proof. Notice that for $u,\, v \in \mathcal{W}_0^1(\Lambda)$, we have

$$\int_\Lambda u x^{-1} \, \partial_x (u x^{-1}) \, \mathrm{d}x = 0,$$

and

$$\big(\partial_x u, \partial_x (v x^{-1})\big) = \int_\Lambda \partial_x (u x^{-1}) \, \partial_x (v x^{-1}) \, x \, \mathrm{d}x + \int_\Lambda u x^{-1} \, \partial_x (v x^{-1}) \, \mathrm{d}x.$$

The desired results then follow from the above and the Cauchy–Schwarz inequality. ∎

Thanks to the above lemma, the existence and uniqueness of the problem (5.1) can be proved by the Lax–Milgram lemma.

5.2. GLOFs-II spectral method and numerical analysis. Define the approximation space by

$$W_N^0 = \text{span}\{\psi_n : n = 1, \ldots, N\} \quad \text{with} \ \ \psi_n(x) = \log x \, \mathcal{U}_{n-1}^{1,\beta}(x). \tag{5.6}$$

Note that $\psi_n(1) = 0$. Then the Galerkin spectral method for (5.2) is to find $u_N = \sum_{n=1}^N \tilde{u}_n \psi_n(x)$ such that

$$a(u_N, v) = (f, v)_{x^{-1}} \quad \forall \ v \in W_N^0. \tag{5.7}$$

Setting $\mathbf{u} = (u_1, \ldots, u_N)^t$ and

$$a_{ij} = a(\psi_j, \psi_i), \ A = (a_{ij}); \ f_j = (f, \psi_j)_{x^{-1}}, \ \mathbf{f} = (f_1, \ldots, f_N)^t, \tag{5.8}$$

the scheme (5.7) becomes $A\mathbf{u} = \mathbf{f}$. Note that unlike the usual Galerkin-spectral methods based on the classical orthogonal polynomials, the matrix A is full. However, since usually N is relatively small, this is a not a big issue.

LEMMA 5.2. *For any $\lambda \neq 0$, the problem* (5.2) *(resp., the scheme* (5.7)*) admit a unique solution u (resp., u_N), and it holds that*

$$\|u - u_N\|_{1,x} \leq \max\{\lambda^{-2}, \lambda^2\} \inf_{v \in W_N^0} \|u - v\|_{1,x}.$$

Proof. We derive from (5.2) and (5.7) that

$$a(u - u_N, v) = 0 \quad \forall \ v \in W_N^0.$$

Then

$$\begin{aligned} \min\{1, \lambda^2\} \|u - u_N\|_{1,x}^2 &\leq a(u - u_N, u - u_N) = a(u - u_N, u - v) \\ &\leq \max\{1, \lambda^2\} \|u - u_N\|_{1,x} \|u - v\|_{1,x} \, \forall v \in W_N^0. \end{aligned}$$

Namely,

$$\|u - u_N\|_{1,x} \leq \frac{\max\{1, \lambda^2\}}{\min\{1, \lambda^2\}} \min_{v \in W_N^0} \|u - v\|_{1,x},$$

which implies the desired result. ∎

For any $\delta > 0$, we define

$$T_\delta u := x^{2+\delta} \partial_x (u x^{-1}), \ u \in \mathcal{W}_0^1(\Lambda). \tag{5.9}$$

LEMMA 5.3. *Let $\beta > 1$ and $\delta > 0$. If $u \in \mathcal{W}_0^1(\Lambda)$ and $T_\delta u \in L^2_{x^{-1}}(\Lambda)$, then*

$$\min_{v \in W_N^0} \|u - v\|_{1,x} \leq C_{\delta,\beta} \|\pi_N^{0,\beta-\delta}\{T_\delta u\} - T_\delta u\|_{x^{-1}},$$

where

$$C_{\delta,\beta} = \left(\left(1 + \frac{\sqrt{\beta + 1}}{2\sqrt{1 + \delta}} \right)^2 + \frac{\left(\sqrt{\beta} + \sqrt{\delta} \right)^2}{4(1 + \delta)\delta\beta} \right)^{1/2}.$$

Proof. Given $u \in \mathcal{W}_0^1(\Lambda)$ and $T_\delta u \in L^2_{x^{-1}}(\Lambda)$, we define

$$\tilde{v}(x) := -\int_x^\infty s^{-2-\delta}\pi_N^{0,\beta-\delta}\{s^{2+\delta}\partial_s(us^{-1})\}\mathrm{d}s, \quad v(x) := x\tilde{v}(x) - \tilde{v}(1)x^{-\beta}.$$

We can show by repeating the integration by parts formula that

$$\tilde{v}(x) = \sum_{j=0}^N c_j \int_x^\infty s^{-\beta-2}[\log s]^j \mathrm{d}s = \sum_{j=0}^N d_j x^{-\beta-1}[\log x]^j,$$

where c_j and d_j are constants. We then find from the above and $v(1) = 0$ that $v \in W_N^0$.

By direct calculation, we find

$$\begin{aligned}
|u-v|_{1,x} &= |u - x\tilde{v} + \tilde{v}(1)x^{-\beta}|_{1,x} \le |u - x\tilde{v}|_{1,x} + |\tilde{v}(1)x^{-\beta}|_{1,x} \\
&= \left(\int_\Lambda \left[\partial_x(ux^{-1}) - \partial_x\tilde{v}\right]^2 x\,\mathrm{d}x\right)^{1/2} + \sqrt{\frac{\beta+1}{2}}|\tilde{v}(1)| \\
&= \left(\int_\Lambda \left[x^{-2-\delta}T_\delta u - x^{-2-\delta}\pi_N^{0,\beta-\delta}\{T_\delta u\}\right]^2 x\,\mathrm{d}x\right)^{1/2} + \sqrt{\frac{\beta+1}{2}}|\tilde{v}(1)| \\
&\le \|\pi_N^{0,\beta-\delta}\{T_\delta u\} - T_\delta u\|_{x^{-1}} + \sqrt{\frac{\beta+1}{2}}|\tilde{v}(1)|,
\end{aligned} \tag{5.10}$$

and

$$\begin{aligned}
|u-v|_{0,x} &\le |u - x\tilde{v}|_{0,x} + |\tilde{v}(1)x^{-\beta}|_{0,x} \\
&= \left(\int_\Lambda \left[ux^{-1} - \tilde{v}\right]^2 x\,\mathrm{d}x\right)^{1/2} + \frac{1}{\sqrt{2\beta}}|\tilde{v}(1)| \\
&= \left(\int_\Lambda \left(\int_x^\infty s^{-2-\delta}\left[\pi_N^{0,\beta-\delta}\{T_\delta u\} - T_\delta u\right]\mathrm{d}s\right)^2 x\,\mathrm{d}x\right)^{1/2} + \frac{1}{\sqrt{2\beta}}|\tilde{v}(1)| \\
&\le \|\pi_N^{0,\beta-\delta}\{T_\delta u\} - T_\delta u\|_{x^{-1}} \left(\int_\Lambda \int_x^\infty s^{-3-2\delta}\mathrm{d}s x\,\mathrm{d}x\right)^{1/2} + \frac{1}{\sqrt{2\beta}}|\tilde{v}(1)| \\
&\le \frac{1}{\sqrt{2\delta(2+2\delta)}}\|\pi_N^{0,\beta-\delta}\{T_\delta u\} - T_\delta u\|_{x^{-1}} + \frac{1}{\sqrt{2\beta}}|\tilde{v}(1)|.
\end{aligned} \tag{5.11}$$

In addition, since $u(x)x^{-1}|_{x=1}^\infty = 0$, one can derive

$$\begin{aligned}
\tilde{v}(1) &= \int_1^\infty \partial_x(ux^{-1})\mathrm{d}x - \int_1^\infty x^{-2-\delta}\pi_N^{0,\beta-\delta}\{x^{2+\delta}\partial_x(ux^{-1})\}\mathrm{d}x \\
&\le \|\pi_N^{0,\beta-\delta}\{T_\delta u\} - T_\delta u\|_{x^{-1}} \left(\int_\Lambda x^{-3-2\delta}\mathrm{d}x\right)^{1/2} \\
&= \frac{1}{\sqrt{2+2\delta}}\|\pi_N^{0,\beta-\delta}\{T_\delta u\} - T_\delta u\|_{x^{-1}}.
\end{aligned} \tag{5.12}$$

The desired result follows by combining the inequalities (5.10)–(5.12). ∎

Combining the above lemmas with the projection estimate (4.10) shown in Theorem 4.1, it is straightforward to obtain the following error estimate.

THEOREM 5.1. *Given $\delta > 0$ and $\tilde{\beta} = \beta - \delta > 1$. We assume $T_\delta u \in L^2_{x^{-1}}(\Lambda)$. If $\mathcal{D}^k_{\tilde{\beta}} T_\delta u \in L^2_{\chi^{k,\tilde{\beta}}}(\Lambda)$ for $k = 0, 1, \ldots, m$, then*

$$\|u - u_N\|_{1,x} \le C_{\delta,\beta,\lambda}\, N^{-\frac{m}{2}} \|\mathcal{D}^m_{\tilde{\beta}} T_\delta u\|_{\chi^{m,\tilde{\beta}}}, \tag{5.13}$$

where $\mathcal{D}_{\tilde{\beta}} = (2\tilde{\beta})^{-1} x^{\tilde{\beta}+1} \partial_x (x^{-\tilde{\beta}} u)$, and for $N \gg 1$,

$$C_{\delta,\beta,\lambda} \approx \max\{\lambda^{-2}, \lambda^2\} \left(\left(1 + \sqrt{\frac{\beta+1}{2}} \right)^2 + \frac{1}{2+2\delta} \left(1 + \frac{1}{\sqrt{2\delta}} \right)^2 \right)^{1/2}.$$

Remark 5.1. In the above error estimate, δ is a tunable parameter for the asymptotic behavior of the underlying solution u. For example, if $u(x)$ behaves like x^{-r}, $r > 0$, at infinity, one should choose $\delta < r$ such that $T_\delta u \in L^2_{x^{-1}}(\Lambda)$.

5.3. Numerical examples. We first take $f(x) = e^{-x}$ for which the exact solution of (5.1) is unknown. We plot the numerical solutions of the problem (5.2) with different $\lambda = 10^{-2}, 10^{-1.5}, 10^{-1}$ in the left of Figure 5.1. We observe that the parameter λ determines the asymptotic behavior of the solution $u_N(x)$. We also plot $\log u_N(x)$ in the right of Figure 5.1, which indicates that the asymptotic behavior of the solution behaves like $e^{-\lambda x}$, which is the eigenfunction of $\partial_{xx} u = \lambda^2 u$.

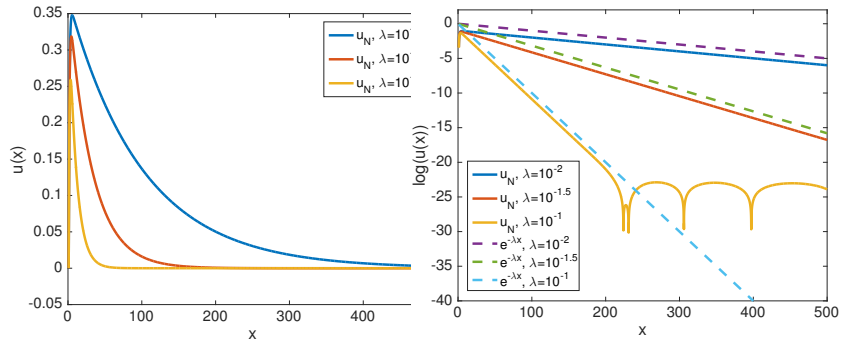

FIG. 5.1. *Solutions of* (5.2) *with different* $\lambda = 10^{-2}, 10^{-1.5}, 10^{-1}$.

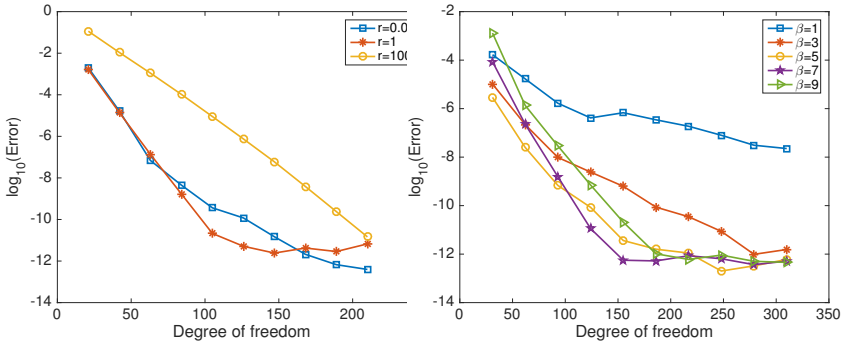

FIG. 5.2. *Convergence curves: L^∞ error.*

Next, we set as the exact solution of the problem (5.1)

$$u(x) = x^{-0.5} - e^{-r(x-1)}, \quad x \in (1, \infty).$$

The convergence curves with $\alpha = 0$, $\beta = 5$, and $r = 0.01, 1, 100$ shown on the left of Figure 5.2 demonstrate that the GLOFs-II spectral methods are very efficient for solving problems with slow algebraic decay and with slow/fast exponential decays. With a fixed $r = 0.01$, the convergence curves plotted in the right graph of Figure 5.2 show that the GLOFs-II are efficient in a wide range of β.

6. Application to fractional differential equations (FDEs). Let $s \in (1, 2)$. We consider the FDEs

$$-{}_xD^s_\infty u + Ku = f, \quad x \in \Lambda = (1, \infty); \quad u(1) = \lim_{x\to\infty} u(x) = 0, \tag{6.1}$$

where the constant $K \geq 0$ and the operator ${}_xD^\nu_\infty$ with $\nu \in (n-1, n)$, $n \in \mathbb{N}^+$, is the Riemann–Liouville fractional derivative defined by

$${}_xD^\nu_\infty u := (-1)^n \frac{\mathrm{d}^n}{\mathrm{d}x^n} {}_xI^{n-\nu}_\infty u, \quad {}_xI^{n-\nu}_\infty u := \frac{1}{\Gamma(n-\nu)} \int_x^\infty \frac{u(t)}{(t-x)^{\nu-n+1}} \mathrm{d}t.$$

Note that if $u^{(k)} \in L(\Lambda)$, $k = 0, 1, \ldots, n$, then

$${}_xD^\nu_\infty u = \frac{(-1)^n}{\Gamma(n-\nu)} \frac{\mathrm{d}^k}{\mathrm{d}x^k} \int_x^\infty \frac{u^{(n-k)}(t)}{(t-x)^{\nu-n+1}} \mathrm{d}t. \tag{6.2}$$

Hence, a weak formulation of the above FDE is to find $u \in H^1_0(\Lambda)$ such that

$$b_s(u, v) = \left({}_xI^{2-s}_\infty u', (vx^{-1})'\right) + K(u, v)_{x^{-1}} = (f, v)_{x^{-1}} \quad \forall v \in H^1_0(\Lambda). \tag{6.3}$$

The corresponding spectral method using GLOFs-II is to find $u_N \in W^0_N$ such that

$$b_s(u_N, v) = (f, v)_{x^{-1}} \quad \forall\, v \in W^0_N, \tag{6.4}$$

where W^0_N is defined as in (5.6).

Remark 6.1. The inner product involving ${}_xI^{2-s}_\infty$ can be computed by

$$\begin{aligned} ({}_xI^{2-s}_\infty g, h) &= \int_1^\infty \frac{1}{\Gamma(2-s)} \int_x^\infty \frac{g(t)}{(t-x)^{s-1}} \mathrm{d}t\; h(x) \mathrm{d}x \\ &= \frac{1}{\Gamma(2-s)} \int_1^\infty k(g, x)\; h(x) \mathrm{d}x, \end{aligned} \tag{6.5}$$

where the function

$$k(g, x) := \int_0^\infty y^{1-s}\; g(y+x) \mathrm{d}y = \int_0^1 y^{1-s} g(y+x) \mathrm{d}y + \int_1^\infty y^{1-s} g(y+x) \mathrm{d}y.$$

The inner integral in the above can be well approximated by shifted Jacobi–Gauss quadrature formula [4, 9, 20, 23, 32, 37, 41] and the outer integral can be well approximated by the Gauss quadrature formula corresponding to GLOFs-II (4.4).

The following fractional derivative relations shown in [31, Table 9.3.1] and [24, Property 2.5] are useful:

$${}_xD^\nu_\infty e^{-rx} = r^\nu e^{-rx}, \quad {}_xD^\nu_\infty x^{-r} = \frac{\Gamma(r+\nu)}{\Gamma(r)} x^{-r-\nu}, \quad [\nu] + 1 - \nu - r < 0. \tag{6.6}$$

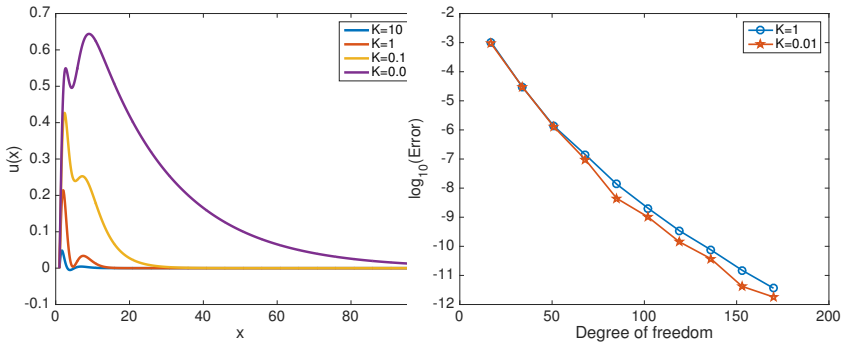

FIG. 6.1. *Left: Solution profiles with* $f(x)=(x-1)(x-3)(x-7)e^{-x}$. *Right: Convergence curves measured by* L^∞ *norm.*

We take $f(x)=(x-1)(x-3)(x-7)e^{-x}$ and plot the numerical solutions of (6.4) with $K=10,1,0.1,0.01$ on the left of Figure 6.1. We observe that, similar to the classical derivative relation $(e^{-\lambda x})''=\lambda^2 e^{-\lambda x}$, the fractional derivative relation (6.6) determines the asymptotic behavior of the problem (6.1). We also plot the convergence curves with $K=1$ and $K=0.01$ ion the right of Figure 6.1, and exponential convergences are observed.

7. Application to the Thomas–Fermi equation (TFE). In the last example, we consider the nonlinear Thomas–Fermi equation, which describes the electrostatic potential associated with the Thomas–Fermi atom model in quantum mechanics [14, 40]. Its normalized form can be read as

$$\partial_{yy}u=\sqrt{u^3/y},\quad y\in(0,\infty), \tag{7.1}$$

which is subjected to the boundary conditions

$$u(0)=1,\quad u(\infty)=0.$$

Remark 7.1. Combining the equation (7.1) with the boundary conditions, one can determine the asymptotic behavior near $y=0$ and at infinity:

$$\lim_{y\to 0}u(y)=1+\lim_{y\to 0}\mathcal{O}(y^{3/2}),\qquad \lim_{y\to\infty}u(y)=\lim_{y\to\infty}\mathcal{O}(y^{-3}).$$

In fact, thanks to [3, eq. (2)] (and the references therein), the exact behavior of the solution u at origin $y=0$ can be expanded as

$$u(y)=1+ay+\frac{4y^{3/2}}{2}+\frac{2ay^{5/2}}{5}+\frac{y^3}{3}+\dots,$$

where $a=u'(0)<0$ is the unknown slope at the origin. On the other hand, we find from [6, 13, 25] that the asymptotic behavior at infinity is

$$u(y)\equiv\frac{144}{y^3}\left(1-\frac{F}{y^\lambda}+0.62569\frac{F^2}{y^{2\lambda}}+\dots\right),$$

where $F=13.27094$ and $\lambda=(\sqrt{73}-7)/2$.

Most classical numerical methods will have trouble accurately handling the singularity near $y=0$ and the algebraic decay at infinity. On the other hand, GLOFs-II are able to efficiently treat the algebraic decay functions but would fail in resolving the weak singularity near $y=0$. However, the particular form of the weak singularity near $y=0$ can be easily handled with a transform [6, 15, 26]. Specifically, setting

$$z=\sqrt{y}, \quad w(z)=u(z^2),$$

the Thomas–Fermi equation (7.1) can be recast as

$$-z\partial_{zz}w+\partial_z w+4z^2w^{\frac{3}{2}}=0; \quad w(0)=1,\ w(\infty)=0. \tag{7.2}$$

Then, the transformed solution $w(z)$ becomes regular at $z=0$.

Using the Newton–Kantorovich iterative method [5, 27, 34], we are led to solve, at each iteration,

$$-z\partial_{zz}w_{k+1}+\partial_z w_{k+1}+6z^2(w_k)^{1/2}w_{k+1}=4z^2(w_k)^{3/2}, \quad w_{k+1}(0)=1,\ w_{k+1}(\infty)=0,$$

whose weak form is

$$b(w_{k+1},v):=\big(z\partial_z w_{k+1}-2w_{k+1},\partial_z v\big)+6\big(z^2(w_k)^{1/2}w_{k+1},v\big)=4\big(z^2(w_k)^{3/2},v\big)+2v(0).$$

Notice that the factor z^2 grows quickly as $x\to\infty$. In order to effectively solve the above problem, we define the approximation space consisting of the shifted GLOFs-II:

$$W_N=span\{\psi_n(z+1)\}_{n=0}^N, \quad \psi_n(z+1):=(z+1)^{-1}\mathcal{U}_n^{0,\beta}(z+1),\ z\in\mathbb{R}^+,$$

and construct the following Galerkin spectral method for (7): find $w_{k+1}\in W_N$ s.t.

$$b(w_N^{k+1},v)=4\big(z^2(w_k)^{3/2},v\big)+2v(0) \quad \forall v\in W_N.$$

An initial guess $w_N^0\in W_N$ can be obtained by solving the linearized equation.

In Figure 7.1, we plot the profile of the numerical solution $u_N(y)$ and its expansion (in GLOFs-II) coefficients. The exponential decay of the coefficients indicates that the numerical error also converges exponentially.

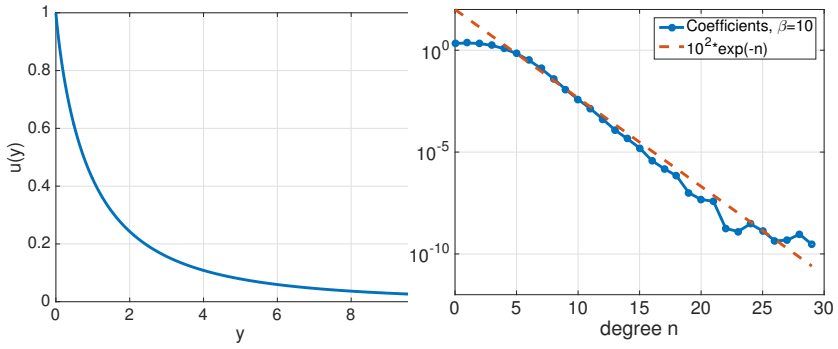

FIG. 7.1. *Left: Solution to TFE. Right: Coefficients behavior.*

8. Concluding remarks. We constructed in this paper two new classes of log orthogonal functions which are suitable for problems which exhibit slow decays at infinity. The log orthogonal functions LOFs-II and GLOFs-II are mutually orthogonal in $L^2_{\chi^\alpha}(\Lambda)$ and $L^2_{\chi^{\alpha,\beta}}(\Lambda)$, respectively, with $\chi^\alpha = (\log x)^\alpha$, $\chi^{\alpha,\beta}(x) = x^{-1}(2\beta \log x)^\alpha$, and $\Lambda = (1,\infty)$. In particular, $u = x^{-r}$ with $r > 1/2$ (resp., $r > 0$) can be well approximated by LOFs-II (resp., GLOFs-II). Furthermore, β in GLOFs-II is a tunable parameter which can be used to adjust the distribution of the log Gauss quadrature nodes (see the left of Figure 4.1). Hence, GLOFs-II are preferred in practice.

Both the theoretical estimates and numerical results showed that GLOFs-II provide uniformly good exponential convergence for problems with slow but monotonic decay solutions at infinity such as x^{-r} or $e^{-\lambda x}$ with small r, $\lambda > 0$.

For problems defined in $[a,\infty)$ (resp., $(-\infty,a]$), one can use the shifted GLOFs-II $\phi_{a,n}(x) := \mathcal{U}_n^{\alpha,\beta}(x-a+1)$ (resp., $\mathcal{U}_n^{\alpha,\beta}(-x+a+1)$). Hence, they are particularly useful for problems whose asymptotic decay rates cannot be determined a priori or for problems having multiple algebraic decay rates.

Note that LOFs-II and GLOFS-II cannot be used to approximate functions which do not decay at infinity, such as $\lim_{x\to\infty} u(x) = 1$. For such problems, we can define another class of GLOFs with three parameters α, β, γ as follows:

$$\mathcal{U}_n^{\alpha,\beta,\gamma}(x) = x^\gamma \, \mathcal{U}_n^{\alpha,\beta}(x), \tag{8.1}$$

which are mutually orthogonal in

$$L^2_{\chi^{\alpha,\beta,\gamma}}(\Lambda), \ \chi^{\alpha,\beta}(x) = x^{-2\gamma-1}(2\beta \log x)^\alpha.$$

Hence, for $\lim_{x\to\infty} u(x) = 1$, we can expand it as

$$u(x) = \sum_{n=0}^{\infty} u_n \mathcal{U}_n^{0,\beta,\gamma}(x), \quad \beta > 1, \ \gamma > 0.$$

Appendix A. Codes for GLOFs-II $\mathcal{U}_n^{\alpha,\beta}(x)$, $x \in \Lambda = [1,\infty)$.

A.1. Generalized log orthogonal functions.

```
function  poly = GLOF2(n, alp, bet, x)
y = x. ∧ (−bet);
x = 2 * bet * log(x);
   if n == 0, poly = y; return; end;
   if n == 1, poly = (alp + 1 − x). * y; return; end;
polylst = y; poly = (alp + 1 − x). * y;
   for k = 1 : n − 1
   polyn = ((2 * k + alp + 1 − x). * poly − (k + alp) * polylst)/(k + 1);
   polylst = poly; poly = polyn;
   end
end
```

A.2. Generalized log Gaussian nodes and weights.

$$
\begin{aligned}
&function \quad [x,w] = GLOF2gs(n, alp, bet)\\
&J = diag(2*[0:n-1] + alp + 1) \ldots .\\
&\qquad + diag(-sqrt([1:n-1].*([1:n-1] + alp)), 1) \ldots .\\
&\qquad + diag(-sqrt([1:n-1].*([1:n-1] + alp)), -1);\\
&r = sort(eig(sparse(J)));\\
&x = exp\big(r/(2*bet)\big);\\
&gm = gammaln(n + alp) - log(n + alp) - gammaln(n + 1);\\
&gm = exp(gm);\\
&w = gm/(2*bet)*r./(GLOF2(n-1, alp, bet, x)).\wedge 2;\\
&end
\end{aligned}
$$

REFERENCES

[1] M. Abramowitz, I. A. Stegun, and R. H. Romer, *Handbook of Mathematical Functions with Formulas, Graphs, and Mathematical Tables*, Natl. Bur. Standards Appl. Math. Ser. 55, U.S. Government Printing Office, Washington, DC, 1988.

[2] P. Amore, *Asymptotic and exact series representations for the incomplete gamma function*, Europhys. Lett., 71 (2005), 1.

[3] P. Amore, J. Boyd, and F. Fernández, *Accurate calculation of the solutions to the Thomas-Fermi equations*, Appl. Math. Comput., 232 (2014), pp. 929–943.

[4] C. Bernardi and Y. Maday, *Spectral methods*, Handbook Numer. Anal., 5 (1997), pp. 209–485.

[5] J. Boyd, *Chebyshev and Fourier Spectral Methods*, 2nd ed., Dover, Mineola, NY, 2001.

[6] J. Boyd, *Rational Chebyshev series for the Thomas-Fermi function: Endpoint singularities and spectral methods*, J. Comput. Appl. Math., 244 (2013), pp. 90–101.

[7] J. Boyd, C. Rangan, and P. Bucksbaum, *Pseudospectral methods on a semi-infinite interval with application to the hydrogen atom: A comparison of the mapped Fourier-sine method with Laguerre series and rational Chebyshev expansions*, J. Comput. Phys., 188 (2003), pp. 56–74.

[8] J. P. Boyd, *Spectral methods using rational basis functions on an infinite interval*, J. Comput. Phys., 69 (1987), pp. 112–142, https://doi.org/10.1016/0021-9991(87)90158-6.

[9] C. Canuto, M. Y. Hussaini, A. Quarteroni, and T. Zang, *Spectral Methods: Fundamentals in Single Domains*, Springer, Cham, 2007.

[10] S. Chen and J. Shen, *Log orthogonal functions: Approximation properties and applications*, IMA J. Numer. Anal., 42 (2022), pp. 712–743.

[11] S. Chen, J. Shen, and L. Wang, *Laguerre functions and their applications to tempered fractional differential equations on infinite intervals*, J. Sci. Comput., 74 (2018), pp. 1286–1313.

[12] S. Chen, J. Shen, Z. Zhang, and Z. Zhou, *A spectrally accurate approximation to subdiffusion equations using the log orthogonal functions*, SIAM J. Sci. Comput., 42 (2020), pp. A849–A877, https://doi.org/10.1137/19M1281927.

[13] C. Coulson and N. March, *Momenta in atoms using the Thomas-Fermi method*, Proc. Phys. Soc. Sec. A, 63 (1950), 367.

[14] E. Fermi, *Un metodo statistico per la determinazione di alcune priorieta dell'atome*, Rend. Accad. Naz. Lincei, 6 (1927), p. 32.

[15] F. Fernández, *Comment on series solution to the Thomas-Fermi equation*, Phys. Lett. A, 372 (2008), pp. 5258–5260.

[16] W. Gautschi, *The incomplete gamma functions since Tricomi*, in Tricomi's Ideas and Contemporary Applied Mathematics, Atti dei Convegni Lincei 147, Accademia Nazionale dei Lincei, Rome, Italy, 1998, pp. 203–237.

[17] R. Gorenflo, F. Mainardi, S. Rogosin, and A. Kilbas, *Mittag-Leffler Functions, Related Topics and Applications*, Springer Monogr. Math., Springer, Cham, 2014.

[18] C. Grosch and S. Orszag, *Numerical solution of problems in unbounded regions: Coordinate transforms*, J. Comput. Phys., 25 (1977), pp. 273–295, https://doi.org/10.1016/0021-9991(77)90102-4.
[19] D. Gu and Z. Wang, *Orthogonal Jacobi rational functions and spectral methods on the half line*, J. Sci. Comput., 88 (2021), pp. 1–27.
[20] B. Guo, *Spectral Methods and Their Applications*, World Scientific, Singapore, 1998.
[21] B. Guo, J. Shen, and Z. Wang, *Chebyshev rational spectral and pseudospectral methods on a semi-infinite interval*, Internat. J. Numer. Methods Engrg., 53 (2002), pp. 65–84.
[22] H. Haubold, A. Mathai, and R. Saxena, *Mittag-Leffler functions and their applications*, J. Appl. Math., 2011 (2011), 298628.
[23] J. Hesthaven, S. Gottlieb, and D. Gottlieb, *Spectral Methods for Time-Dependent Problems*, Cambridge Monogr. Appl. Comput. Math. 21, Cambridge University Press, Cambridge, UK, 2007.
[24] A. Kilbas, H. Srivastava, and J. Trujillo, *Theory and Applications of Fractional Differential Equations*, Elsevier, New York, 2006.
[25] S. Kobayashi, S. Nagai, and K. Umeda, *Accurate value of the initial slope of the ordinary tf function*, J. Phys. Soc. Japan, 10 (1955), pp. 759–762.
[26] A. MacLeod, *Chebyshev series solution of the Thomas-Fermi equation*, Comput. Phys. Commun., 67 (1992), pp. 389–391.
[27] V. Mandelzweig and F. Tabakin, *Quasilinearization approach to nonlinear problems in physics with application to nonlinear ODEs*, Comput. Phys. Commun., 141 (2001), pp. 268–281.
[28] M. Mori and M. Sugihara, *The double-exponential transformation in numerical analysis*, J. Comput. Appl. Math., 127 (2001), pp. 287–296.
[29] I. Podlubny, *Fractional Differential Equations: An Introduction to Fractional Derivatives, Fractional Differential Equations, to Methods of Their Solution and Some of Their Applications*, Math. Sci. Engrg. 198, Academic Press, San Diego, CA, 1999.
[30] G. Y. Popov, *Concentration of Elastic Stresses near Punches, Cuts, Thin Inclusions and Supports*, Nauka, Moscow, 1982.
[31] S. Samko, A. Kilbas, and O. Maričev, *Fractional Integrals and Derivatives*, Gordon and Breach Science Publishers, Yverdon, Switzerland, 1993.
[32] J. Shen, T. Tang, and L. Wang, *Spectral Methods: Algorithms, Analysis and Applications*, Springer Ser. Comput. Math. 41, Springer-Verlag, Berlin, Heidelberg, 2011.
[33] J. Shen and L. Wang, *Some recent advances on spectral methods for unbounded domains*, J. Commun. Comput. Phys., 5 (2009), pp. 195–241.
[34] A. Sherman, *On Newton-iterative methods for the solution of systems of nonlinear equations*, SIAM J. Numer. Anal., 15 (1978), pp. 755–771, https://doi.org/10.1137/0715050.
[35] F. Stenger, *Numerical Methods Based on Sinc and Analytic Functions*, Springer Ser. Comput. Math. 20, Springer, New York, 1993.
[36] F. Stenger, *Handbook of Sinc Numerical Methods*, CRC Press, Boca Raton, FL, 2016.
[37] G. Szegö, *Orthogonal Polynomials*, 4th ed., American Mathematical Society Colloquium Publications 23, AMS, Providence, RI, 1975.
[38] H. Takahasi and M. Mori, *Double exponential formulas for numerical integration*, Publ. Res. Inst. Math. Sci., 9 (1974), pp. 721–741.
[39] K. Tanaka, M. Sugihara, K. Murota, and M. Mori, *Function classes for double exponential integration formulas*, Numer. Math., 111 (2009), pp. 631–655.
[40] L. Thomas, *The calculation of atomic fields*, in Math. Proc. Cambridge Philosophical Soc., 23 (1927), pp. 542–548.
[41] L. Trefethen, *Approximation Theory and Approximation Practice*, Extended Edition, SIAM, Philadelphia, 2019, https://doi.org/10.1137/1.9781611975949.
[42] Z. Wang and B. Guo, *Jacobi rational approximation and spectral method for differential equations of degenerate type*, Math. Comput., 77 (2008), pp. 883–907.
[43] X. Zhao, L. Wang, and Z. Xie, *Sharp error bounds for Jacobi expansions and Gegenbauer–Gauss quadrature of analytic functions*, SIAM J. Numer. Anal., 51 (2013), pp. 1443–1469, https://doi.org/10.1137/12089421X.